

1
2
3
4
5
6
7
8
9
10
11
12
13
14
15
16
17
18
19
20
21
22
23
24
25
26
27
28
29
30
31
32
33
34
35
36

Humic surface waters of frozen peat bogs (permafrost zone)
are highly resistant to bio- and photodegradation

Liudmila S. Shirokova^{1,2}, Artem V. Chupakov², Svetlana A. Zabelina²,
Natalia V. Neverova², Dahedrey Payandi-Rolland¹, Carole Causseraund¹,
Jan Karlsson³, Oleg S. Pokrovsky^{1,4*}

¹ *Geoscience and Environment Toulouse, UMR 5563 CNRS, University of Toulouse, 14 Avenue Edouard Belin, Toulouse 31400, France*

² *Institute of Ecological Problems of the North, N. Laverov Federal Center for Integrated Arctic Research, Nab Severnoi Dviny 23, Arkhangelsk 163000, Russia*

³ *Climate Impacts Research Centre (CIRC), Department of Ecology and Environmental Science, Umeå University, 901 87 Umeå, Sweden*

⁴ *BIO-GEO-CLIM Laboratory, Tomsk State University, 35 Lenina Pr., Tomsk 634050, Russia*

*corresponding author email: oleg.pokrovsky@get.omp.eu

Key words: depression, stream, river, organic carbon, photolysis, respiration, palsa, permafrost

Bullet points:

- Low (< 10%) concentration of bio- and photo-degradable DOM in humic waters from frozen peatlands, discontinuous /continuous permafrost zone
- Low importance of biodegradation and photolysis on DOC processing and CO₂ evasion in surface waters of permafrost-affected peatland regions.
- The paradigm of the importance of photolysis and biodegradation in DOC processing in surface waters from permafrost region is challenged for the case of frozen peatlands
- We hypothesize the peat porewater DOM processing and respiration of sediments as main drivers of elevated pCO₂ concentration and emission in humic boreal waters of frozen peat bogs.

Synopsis: We measured very low bio- and photo-degradability of aquatic DOM from frozen Arctic peatland which may require revisiting the current paradigm of the importance of bio- and photodegradation of DOC in permafrost regions; this should be taken into account for pan-Arctic modeling of C biogeochemical cycle in continental waters.

Submitted to *Biogeosciences*, after revision 25 March 2019

37 **Abstract**

38 Bio- and photo-degradation of dissolved organic matter (DOM) is identified as dominant vector
39 of C cycle in boreal and high-latitude surface waters. In contrast to large number of studies of
40 humic waters from permafrost-free regions and oligotrophic waters from permafrost-bearing
41 regions, the bio- and photo-lability of DOM from humic surface waters of permafrost-bearing
42 regions has not been thoroughly evaluated. Following standardized methods, we measured
43 biodegradation (low, intermediate, high temperature) and photodegradation (one intermediate
44 temperature) of DOM in surface waters along the hydrological continuum (depression → stream
45 → thermokarst lake → river Pechora) within a European Russian frozen peatland. In all systems,
46 **within the experimental resolution of 5 to 10%, there was no** bio- or photodegradation of DOM
47 over 1 month of incubation. It is possible that the main cause of the lack of degradation is the
48 dominance of allochthonous refractory (soil, peat) DOM in all studied waters. Yet, all surface
49 waters were supersaturated with CO₂. Thus, this study suggest that, rather than bio- and photo-
50 degradation of DOM in the water column, other factors such as peat porewater DOM processing
51 and respiration of sediments are the main drivers of elevated pCO₂ and emission in humic boreal
52 waters of frozen peat bogs.

53

54 **Introduction**

55 Boreal and subarctic waters contain large amounts of plant, soil, and peat-originated
56 dissolved organic matter (Wilkinson et al., 2013; Kaiser et al., 2017), and the proportion of land-
57 derived organic carbon in waters is likely to increase with ongoing permafrost thaw (Wauthy et
58 al., 2018). Heterotrophic bacteria degrade this DOM (Karlsson, 2007; McCallister and del
59 Georgio, 2008), causing net heterotrophic conditions (Gross Primary Productivity < Respiration)
60 and CO₂ emission to the atmosphere from surface waters (Ask et al., 2012; Lapierre et al., 2013).
61 Between 10% and 40% of the dissolved organic carbon (DOC) in lakes, rivers and soil waters

62 of the boreal zone may be available for bacterial uptake over a time frame of several weeks
63 (Berggren et al., 2010; Roehm et al., 2009). The biodegradability of DOM leached from
64 permafrost and non-permafrost soils was recently reviewed by Vonk et al. (2015) who concluded
65 that aquatic DOC is more biodegradable in regions with continuous permafrost compared to
66 regions without permafrost. At the same time, among all Arctic rivers, the highest annual (20%)
67 and winter (ca. 45%) biodegradable DOC (BDOC) was reported for the Ob River, draining
68 through peatlands with minimal influence of permafrost (Wickland et al., 2012). Further, based
69 on 14 studies of BDOC and their own research, Vonk et al. (2015) demonstrated zero BDOC loss
70 in aquatic systems without permafrost, which is contradictory to general understanding of
71 biodegradation of aquatic DOM as major driver of CO₂ emission in boreal waters. It is also
72 important to note that all the available bio-degradation studies of inland waters in permafrost
73 regions dealt with either tundra ecosystems with shallow peat soils overlaying the mineral
74 substrate or mountain regions with essentially mineral soil substrates in Alaska or Canada
75 (Holmes et al., 2008; Wickland et al., 2012; Ward et al., 2017) and with the yedoma soils of
76 Eastern Siberia (Mann et al., 2014, 2015; Spencer et al., 2015).

77 Similarly, although the photolysis of DOM in boreal and subarctic aquatic environments
78 contributes to CO₂ emission from the inland waters to the atmosphere (Cory et al., 2014), the
79 overwhelming majority of photo-degradation studies in the Arctic were conducted on oligotrophic
80 lake waters and streams draining mineral soils of mountain regions (Ward and Cory, 2016; Cory
81 et al., 2013, 2015). The dominance of photolytic processes in DOM processing in arctic waters
82 was reported for N America (Cory et al., 2014; Ward et al., 2017), Canadian surface waters of
83 the temperate zone (Winter et al., 2007; Porcal et al., 2013, 2014, 2015), and small Swedish
84 humic-rich headwater catchments (Köhler et al., 2002). In contrast, several other studies from
85 Scandinavia (Groeneveld et al., 2016; Koehler et al., 2014), Canada (Laurion and Mladenov,
86 2013; Gareis and Lesack, 2018) and NW Russia (Oleinikova et al., 2017; Chupakova et al., 2018)

87 demonstrated sizeable removal of colored (chromophoric DOM) but quite small ($\leq 10\%$) impact
88 of sunlight irradiation on bulk DOC concentration in streams, rivers and lakes. Note here that the
89 interaction between photo- and bio-degradation is more important than the individual processes
90 as photo-oxidation may transform DOM molecular structures into more bioavailable forms (e.g.,
91 Cory and Kling, 2018; Sulzberger et al., 2019).

92 Overall, available data demonstrate that an emerging paradigm on the importance of bio-
93 and photodegradation may not be as consistent across the Arctic as previously thought, which
94 call a need for further studies of these processes, encompassing wider range of aquatic settings.
95 The numerous surface waters located within discontinuous to continuous permafrost zone of
96 Northern Eurasia, where most aquatic systems are drained through frozen peat rather than mineral
97 substrates, are poorly studied regarding bio- and photo-degradability of aquatic DOM. Yet, these
98 regions (NE European Russia or Bolshezemelskaya tundra, Western Siberia Lowland, Northern
99 Siberian Lowland, Kolyma and Yana-Indigirka Lowland) occupy > 2 million km² which is more
100 than 10% of overall permafrost-affected land area and exhibit, in average, ten times higher
101 concentration of soil organic C in the form of 0.5 to 3 m thick peat layer than the rest of the
102 circumpolar regions (Tarnocai et al., 2009; Raudina et al., 2018). As a result of the dominance
103 of histosols, the surface waters draining frozen peatlands are enriched in DOC compared to other
104 permafrost-affected regions (Manasypov et al., 2014; Pokrovsky et al., 2015) and may provide
105 disproportionally high contribution to overall DOM bio- and photo-degradability in the Arctic
106 and subarctic regions.

107 Numerous experiments in permafrost-bearing and permafrost-free aquatic environments
108 including both organic and mineral soil substrates relatively poor in DOC demonstrated that the
109 headwater streams and soil leachate contain most bio-degradable and photo-degradable DOM
110 (Ilina et al., 2014; Mann et al., 2014, 2015; Larouche et al., 2015; Spencer et al., 2015; Vonk et
111 al., 2015). Photo-oxidation and biodegradation were also shown to play important role in small

112 streams of temperate peatlands of UK and Scotland (Moody et al., 2013; Pickard et al., 2017;
113 Dean et al., 2019). In the present study, we hypothesized that, given nutrient-poor nature of
114 Sphagnum peat from histosols, the bioavailability of essentially recalcitrant DOM in surface
115 waters of frozen peatlands will be low. However, we expected a gradient in the degree of bio-
116 and photo-lability of DOM from permafrost subsidence, head water stream, thermokarst lake and
117 large river, corresponding to the increase in water residence time (Mann et al., 2012).

118 To test these hypotheses, we used recommended standardized protocol for DOM
119 biodegradation (Vonk et al., 2015) and applied it for 4 main aquatic components of a hydrological
120 continuum ‘permafrost subsidence → small stream → large thermokarst lake → large river
121 (Pechora)’. We chose the largest frozen peatlands in Europe, the Bolshezemelskaya Tundra of
122 NE European Russia which is represented by flat-mound (palsa) peat bog (discontinuous and
123 continuous permafrost zone) and belongs to the watershed of the largest European permafrost-
124 affected river, Pechora. Specific questions of this study were (i) to assess the difference in BDOC
125 and photodegradable (PDOC) fraction of DOM in surface waters of frozen peat bog along the
126 hydrological continuum, from permafrost depression to large rivers, (ii) to quantify the impact
127 of temperature on biodegradation potential of surface waters from frozen peatbogs and predict
128 possible impact of warming on DOM biodegradation efficiency, and (ii) to relate the BDOC and
129 PDOC concentrations to the snapshot CO₂ concentration and emission.

130

131

132 2. Study site and methods

133 2.1. Geographical context and hydrological continuum of the Pechora River basin

134 The water samples were collected in the middle of July 2017 which is the middle summer
135 period, consistent with time used by other researchers for biodegradation assays. The
136 BolsheZemelskaya Tundra (BZT) peatland (continuous to discontinuous permafrost zone)

137 belongs to the Pechora River watershed (**Fig. S1**), the largest European Arctic river draining
138 permafrost-bearing terrain (watershed = 322,000 km²; mean annual discharge is 4140 m³/s). The
139 northern part of the Pechora watershed is covered by permafrost: discontinuous on the eastern
140 part and sporadic to isolated on the western part (Brittain et al., 2009). The BZT is a hilly moraine
141 lowland located between rivers Pechora and Usa (from the west and south) and the Polar Ural
142 and Pai-Khoi ridge from the east. The dominant altitudes are between 100 and 150 m, created by
143 hills and moraine ridges, composed of sands and silt with boulders. Between the moraines and
144 ridges there are many lakes, mostly of thermokarst origin. The dominant soils are histosols of
145 peat bogs and podzol-gleys in the southern forest-tundra zone. The mean annual temperature is -
146 3.1°C and the mean annual precipitation is 503 mm. The dominant vegetation of the tundra zone
147 is mosses, lichens and dwarf shrubs. **Over past decades, the lakes of BZT exhibited sizeable**
148 **increase in summer time temperature and pCO₂, presumably due to enhanced bacterial respiration**
149 **of allochthonous DOM from thawing permafrost (Drake et al., 2019).**

150 We sampled surface waters along the typical hydrological continuum **shown in Fig. S1**
151 **and** consisting of 1) depression in the moss and lichen cover of upland frozen peat bog, filled by
152 water from thawing of ground ice (permafrost subsidence, 2.5 x 3 m size and 0.3 m depth); 2)
153 small stream (~2 km length) originated from upland peat bog; 3) small thermokarst lake Isino
154 (S_{area} = 0.005 km²) located within the peat bog, and 4) the Pechora River mainstream. Similar
155 principle of the hydrological continuum was considered in the Kolyma River biodegradation
156 experiments (Mann et al., 2012). The list of sampled water objects together with their physical,
157 chemical, **microbiological** characteristics and parameters of CO₂ system is presented in **Table 1**.
158 The surface waters were collected from the shore (depression and stream) or the PVC boat (r.
159 Pechora and Lake Isino). The water samples were placed into 2-L Milli-Q pre-cleaned PVC jars
160 and kept refrigerated until arrival to the laboratory, within 2-3 h after collection.

161

162 2.2. *Experimental set-up*

163 2.2.1. Biodegradation

164 For biodegradation assays we followed the standardized protocol for assessing
165 biodegradable DOC of Arctic waters (Vonk et al., 2015). To facilitate the implementation of
166 recommended protocol, we used exactly the same filter towers, inline filter holders, and vacuum
167 devices as depicted in Vonk et al. (2015). Initial samples were filtered through pre-combusted
168 (4.5 h at 450°C) Whatman GF/F filters of nominal poresize 0.7 µm. All the manipulations were
169 performed in laminar hood box (class A100) under sterile environment; the working space was
170 sterilized by UV light before preparation. Triplicate 30 mL aliquots of 0.7 µm-filtered water were
171 placed into pre-combusted (4.5 h at 450°C) dark borosilicate glass bottles of 40 mL volume
172 wrapped in Al foil to prevent any photolysis, without nutrient amendment and stored at 23±1°C
173 in the dark in thermostat. The bottles were closed with sterilized PVC caps. As recommended,
174 the caps were left loose and the bottles were shaken manually once a day avoiding the liquid
175 touching the cap. The incubated samples were re-filtered through pre-combusted 0.7 µm GF/F
176 filters using sterilized dismountable Sartorius 25 mm filter holder and a cleaned sterile syringe
177 after 0, 2, 7, 14 and 28 days of exposure. All handling and sampling of bottles was performed in
178 the laminar hood box under sterilized workspace. Filtered samples were acidified with 30 µL of
179 concentrated (8.1 M) double distilled HCl, tightly capped and stored in the refrigerator before
180 DOC analyses. Non-acidified portion of filtrate was used for pH, Specific Conductivity, DIC and
181 UV_{254nm} and optical spectra measurement. Control runs were 0.22 µm sterile-filtered water which
182 was incubated in parallel to experiments and re-filtered through 0.7 µm GF/F filters at the day of
183 sampling.

184 In addition to this ‘classic’ protocol, we used alternative procedure of biodegradation
185 experiments to test maximally possible DOM removal by bacteria. For this, we replaced initial
186 0.7 µm GF/F filtration by 3 µm filtration through sterilized Nylon Sartorius membranes, to

187 increase the amount of bacterial cells capable to degrade DOM during incubation. The reason for
188 that is that conventional 0.7 μm (GF/F) filtration might remove too many microbial cells (Dean
189 et al., 2018). Besides, re-filtration through the same filter pore size (0.7 μm) recommended in
190 classic protocol may not necessarily remove the newly formed microbial biomass as the cell size
191 of bacteria grown during incubation may not exceed 0.7 μm . In this regard, initial 3 μm -filtration
192 is equivalent of 100% inoculum used by Vonk et al. (2015) and can be considered as maximal
193 enhancement of DOM biodegradation without addition of nutrients. Further, instead of 0.7 μm
194 refiltration for sampling, we employed 0.22 μm filter pore size for DOC samplings during
195 incubation. This allowed to remove all particulate organic carbon formed via microbial
196 metabolism, as well as some newly grown microbial cells and therefore should enhance the
197 degree of biodegradation calculated as the difference between initial 3 μm -filtration and 0.22 μm
198 filtration at the date of sampling. The control runs were filtered through sterile 0.22 μm filters
199 and incubated parallel to the experiments, following the standard approach for control abiotic
200 experiments in incubation experiments (Köhler et al., 2002). They were re-filtered through 0.22
201 μm membrane at the day of experimental sampling. To insure the lack of DOC release from
202 sterilized Nylon membrane, we run blank (Milli-Q) filtration through both 0.7 μm GF/F and 0.22
203 μm Nylon filters; in both cases the DOC blank was below 0.1-0.2 mg/L which is less than 1% of
204 DOC concentration in our samples. The glass bottles were incubated in triplicates at $4\pm 2^\circ\text{C}$,
205 $22\pm 1^\circ\text{C}$ and $37\pm 3^\circ\text{C}$ using refrigerator and incubators and agitated manually at least once a day
206 over 4 weeks of exposure.

207

208 2.2.2. Photodegradation

209 For photodegradation incubations, water samples of all sites except the river were
210 collected in polypropylene jars and sterile filtered (0.22 μm Nalgene Rapid-Flow Sterile
211 Systems) within 2 h of sampling and refrigerated. The filtrates were transferred under laminar

212 hood box into sterilized, acid-washed quartz tubes (150 mL volume, 20% air headspace) and
213 placed at 3 ± 2 cm depth into outdoor pool which was filled by river water having the light
214 transparency similar to that of the Pechora River (1.5-2.0 m Secchi depth). In-situ measurements
215 of sunlight intensity were conducted using submersible sunlight sensor. The outdoor pools were
216 placed under unshaded area, at the latitude similar to that of the sampling sites. Slight wind
217 movement and regular manual shaking allowed for sufficient mixing of the interior of reactors
218 during exposure. All the experiments were run in triplicates. The water temperature was $19\pm 3^{\circ}\text{C}$
219 over 28 days of exposure (17 July - 14 August 2017), with an average magnitude of diurnal water
220 temperature variation of 6°C (recorded every 3 h using EBRO EBI 20 Series loggers). The day
221 light intensity was typically between 5,000 and 20,000 lux (in average 10,000 lux or $14\pm 5 \text{ W/m}^2$)
222 which is within the range of solar radiation at the latitude of the polar circle during this period of
223 the year. Overall, we followed conventional methodology for photodegradation which is
224 exposure of $0.2 \mu\text{m}$ -sterile filtered samples in quartz reactors in the outdoor pool (Vähätalo et al.,
225 2003; Chupakova et al., 2018; Gareis and Lesack, 2018), solar simulator (Lou and Xie, 2006;
226 Amado et al., 2014) or directly in the lake water (Laurion and Mladenov, 2013; Groeneveld et
227 al., 2016). Note that the $0.22 \mu\text{m}$ sterile filtration is the only way of conducting photodegradation
228 experiments, given that the autoclave sterilization of DOM-rich natural water would coagulate
229 humic material and thus is not suitable (Andresson et al., 2018). We have chosen 4 weeks
230 exposure time for consistency with biodegradation experiments described above and following
231 the previous studies on photodegradation under sunlight, which is typically from 15 to 70 days
232 (Moran et al., 2000; Vähätalo and Wetzel, 2004; Mostofa et al., 2007; Helms et al., 2008;
233 Chupakova et al., 2018). Dark control experiments were conducted in duplicates, using sterilized
234 glass tubes filled by sterile $0.22 \mu\text{m}$ -filtered water, wrapped in Al foil and placed in the same
235 outdoor pool as the experiments. The headspace (approx. 20% of total reaction volume) was
236 similar in experimental and control reactors. The individual reactors were sterile sampled at the

237 beginning and at the 2nd, 7th, 14th, 21th and 28th day of exposure. Each sampling sacrificed the
238 entire reactor. The MilliQ blanks were collected and processed to monitor for any potential
239 sample contamination introduced by our filtration, incubation, handling and sampling
240 procedures. The organic carbon blanks of filtrates never exceeded 0.2 mg/L.

241

242

243 *2.3. Analyses and treatment*

244 The temperature, pH, O₂ and specific conductivity in surface waters were measured in
245 the field as described previously (Shirokova et al., 2013b). Dissolved CO₂ concentration was
246 measured using submersible Vaissala Carbocap® GM70 Hand-held carbon dioxide meter with
247 GMP222 probes (accuracy 1.5%; see Serikova et al. (2018, 2019) for methodological details).
248 The diffusional CO₂ flux was calculated using wind-based model (Cole and Caraco, 1998) with
249 $k_{600} = 2.07 + 0.215 \times u_{10}^{1.7}$, where u_{10} is the wind speed at 10 m height. In the filtrates, we measured
250 optical density at 254 nm and at selected wavelengths (365, 436, 465, and 665 nm) of the visible
251 spectrum. The specific UV-absorbency (SUVA₂₅₄, L mg⁻¹ m⁻¹) and E4:E6 ratios are used as a
252 proxy for aromatic C, molecular weight and source of DOM (Weishaar et al., 2003; Peacock et
253 al., 2013; Ilina et al., 2014).

254 The DOC and DIC were analyzed by high-temperature catalytic oxidation using TOC-
255 VCSN, Shimadzu® (uncertainty ± 2%, 0.1 mg L⁻¹ detection limit). The DIC was measured after
256 sample acidification with HCl and DOC was analyzed in acidified samples after sparging it with
257 C-free air for 3 min at 100 mL min⁻¹ as non-purgable organic carbon (NPOC). Selected quartz
258 reactors in photodegradation experiments were used to measure dissolved O₂ using Oxi 197i
259 oximeter with a Cellox® 325 galvanic submersible sensor (WTW, Germany; ± 0.5%
260 uncertainty). For this, the O₂ galvanic sensor was introduced into the quartz tube immediately

261 after opening of the reactor and allowed to equilibrate for 5-10 min while protecting the open
 262 end of the tube from the exchange with atmospheric oxygen via wrapping it in Al foil. All filtered
 263 samples collected from photo-degradation experiments were acidified with ultrapure nitric acid
 264 and analyzed for major and trace elements following procedures employed in GET (Toulouse)
 265 for analyses of boreal humic waters (Oleinikova et al., 2017, 2018).

266 To account for possible microbial development in biodegradation experiments, we
 267 performed oligotrophic and eutrophic bacteria count in the course of incubation, following the
 268 standard methodology used in biodegradation experiments of peat waters (Stutter et al., 2013) as
 269 also described previously (Shirokova et al., 2017b; Chupakova et al., 2018). In addition, we
 270 measured total bacterial number and quantified the dominant cell size morphology using DAPI
 271 fluorescence method (Porter and Feig, 1980). Control experiments did not demonstrate the
 272 presence of any countable cells in the observation fields.

273 The bio- and photodegradable DOC (BDOC and PDOC, respectively) were calculated in
 274 percent loss relative to control at each sampling time point t (0, 2, 7, 14 and 28 days) according
 275 to:

$$276 \quad \text{BDOC}(\%)_t = 100\% \times (\text{DOC}_{t, \text{control}} - \text{DOC}_t) / \text{DOC}_{t, \text{control}} \quad (1)$$

277 Alternatively, the BDOC and PDOC were calculated in percent loss at time point t relative to the
 278 initial concentration of DOC ($\text{DOC}_{t=0}$) following Vonk et al. (2015):

$$279 \quad \text{BDOC}(\%)_t = 100\% \times (\text{DOC}_{t=0} - \text{DOC}_t) / \text{DOC}_{t=0} \quad (2)$$

280 For most treatments and sampled waters, the difference between two methods of bio-
 281 /photodegradable DOC concentration was statistically negligible. To assess the variability of
 282 results, shown as vertical uncertainties in the graphs, we used the percentage ratio of standard
 283 deviation of n replicates at the i -th day of exposure to the initial DOC concentration following:

$$284 \quad SD_i = \sqrt{\frac{(\text{BDOC}_i^1 - \text{BDOC}_i^{\text{mean}})^2 + (\text{BDOC}_i^2 - \text{BDOC}_i^{\text{mean}})^2 + \dots + (\text{BDOC}_i^n - \text{BDOC}_i^{\text{mean}})^2}{n}} \quad (3)$$

285
$$\%SD_i = \frac{SD_i}{DOC_0} \cdot 100 \quad (4)$$

286 The results are presented as % $BOD_i \pm SD_i$.

287 To assess the uncertainties during photodegradation experiments, we used the percentage of
 288 standard deviation on n replicates at the i -th day of exposure to the DOC concentration in the
 289 dark (control) reactors as

290
$$PDOC_i^n = DOC_i^{blank} - DOC_i^n \quad (5)$$

291
$$PDOC_i^{mean} = \frac{PDOC_i^1 + PDOC_i^2 + \dots + PDOC_i^n}{n} \quad (6)$$

292
$$\%PDOC_i = \frac{PDOC_i^{mean}}{DOC_i^{blank}} \cdot 100 \quad (7)$$

293
$$SD_i = \sqrt{\frac{(PDOC_i^1 - PDOC_i^{mean})^2 + (PDOC_i^2 - PDOC_i^{mean})^2 + \dots + (PDOC_i^n - PDOC_i^{mean})^2}{n}} \quad (8)$$

294
$$\%SD_i = \frac{SD_i}{DOC_i^{blank}} \cdot 100 \quad (9)$$

295 The results are presented as % $PDOC_i \pm SD_i$

296 Note that in case of negative values provided by Eqn. 2, the BDOC was taken as 0% following
 297 the conventional practice in biodegradation experiments (Vonk et al., 2015). The uncertainties
 298 of BDOC % numbers were between ± 5 and $\pm 10\%$ for experiments, at 4, 23 and 37°C using
 299 modified (3 μm and 0.22 μm filtration) protocol. In ‘classic’ protocol (0.7 μm GF/F filtration)
 300 the uncertainties were as high as 10-15% at the end of experiment. We believe that such high
 301 uncertainties are linked to high initial DOC concentration, triplicate measurements and
 302 simultaneous monitoring of experimental and control runs.

303 Statistical treatment included the least squares method and the Pearson correlation,
 304 because the data were normally distributed. The ANOVA method was used to test the differences
 305 in the average DOC concentration versus time in incubation experiments and in the controls and
 306 to assess the difference between the light experiments and the dark control for photo-degradation

307 experiments. All calculations were performed in STATISTICA ver. 10 (StatSoft Inc.,Tulsa) at p
308 = 0.05).

309

310

311

312 **3. Results**

313 *3.1. Assessment of biodegradable DOC*

314 The waters of hydrological continuum within the Pechora River basin are highly diverse
315 (**Table 1**), with pH range from 3.8 (frozen peat depression) to 6.9 (r. Pechora). The soluble salts
316 concentrations are low as the specific conductivity ranged from $20\pm 10 \mu\text{S cm}^{-1}$ (stream,
317 thermokarst lake) to $\sim 60 \mu\text{S cm}^{-1}$ in the peat bog depression and the Pechora River. The DOC
318 concentration decreased from 44 mg/L in frozen peat depression to ~ 8 mg/L in the Pechora River
319 following the order of water residence time (flow direction) “depression \gg stream \geq thermokarst
320 lake $>$ r. Pechora”. The DOC concentration was generally similar (within $\pm 2\%$) between 3, 0.7
321 and 0.22 μm pore size filtration of the initial sample, in agreement with former size fractionation
322 measurement in Arctic and subarctic systems (Vasyukova et al., 2010; Pokrovsky et al., 2012,
323 2016). All sampled surface waters exhibited CO_2 supersaturation with respect to atmosphere
324 (from 440 to 2400 ppm) and net CO_2 emission (diffusion) flux ranging from 34 to 74 mmol CO_2
325 $\text{m}^{-2} \text{d}^{-1}$ (**Table 1**).

326 In both protocols of biodegradation experiments, two major features were noted: (1) the
327 concentrations of 0.7 μm and 0.22 μm -filtered DOC did not decrease during the exposure and
328 (2) there was no sizable ($> 10\%$) difference between the control run and the incubation
329 experiment (**Fig. 1**). By ‘classic’ protocol of biodegradation experiments (0.7 μm GF/F filtration)
330 at 23°C, the BDOC fraction ranged between 0 and 10 % for all surface waters. The modified
331 procedure (3 μm initial filtration and 0.22 μm sampling) did not detect any significant

332 biodegradation for any of the studied waters (average equaled to $5\pm 5\%$ at 4, 23 and 37°C , **Fig. 2**
333 **B, C, D**). The DIC concentrations remained constant ($\pm 5\%$ of the initial value) in all experiments,
334 but increased in stream water incubated at 37°C , where we measured $\sim 10\%$ increase over 28 days
335 of exposure (not shown). This increase was equal to 0.2 mg/L of DIC. Note that equivalent
336 decrease in DOC concentration could not be assessed, presumably due to instrument limitation
337 (the intrinsic uncertainty on NPOC analyses (ca. 2% of 15 mg/L of DOC) which did not allow
338 measuring C change smaller than 0.3 mg/L .

339 The $\text{UV}_{254\text{ nm}}$ absorbency of samples in the course of dark aerobic exposure demonstrated
340 slight decrease with time (ca., between 5 and 10% over 28 days) in peat bog depression by
341 ‘classic’ protocol (**Fig. S2 of Supplement**). However, in all other treatments, the control was
342 indistinguishable from experimental runs and the SUVA_{254} remained constant within the
343 uncertainties of triplicates (ca., ± 5 to $\pm 10\%$). Similarly, no measurable change in optical
344 properties of DOM (absorbency at 365, 465, 665 nm and E4:E6 ratio) could be detected during
345 exposition.

346 The microbial consortium of all systems was dominated by cocci ($0.23\text{ }\mu\text{m}$ median size)
347 and rods ($0.96 \times 0.20\text{ }\mu\text{m}$) as revealed from DAPI fluorescent imaging. The number of culturable
348 oligotrophic bacteria increased by a factor of ~ 100 after first 2-7 days of exposure at 22°C both
349 in GF/F-filtered and $3\text{ }\mu\text{m}$ -filtered samples, and then remained stable at ca. $10,000$ to $20,000\text{ CFU}$
350 mL^{-1} till the end of experiments (**Fig. S3 A, C**). The highest concentration of oligotrophic bacteria
351 was observed in the Pechora River, where as the other samples were not significantly different
352 between each other. The CFU value at 4°C ranged between 1000 and 5000 CFU mL^{-1} and did
353 not demonstrate any clear pattern with time of incubation (**Fig. S3 B**). The number of eutrophic
354 bacteria ranged between $1,000$ and $15,000\text{ CFU mL}^{-1}$ following the order: r. Pechora $>$ stream \geq
355 peat bog depression \geq thermokarst lake. There was no growth of eutrophic or oligotrophic
356 bacteria at 37°C . The total cell number gradually increased in the course of experiment at 22°C

357 (Fig. S3 D) with maximal changes observed in peatbog depression and the Pechora River (by a
358 factor of 30 and 40, respectively). There was a progressive increase of rod-shaped bacillus
359 relative to coccus in the Pechora River and a permafrost stream whereas the thermokarst lake and
360 peatbog depression did no exhibit any systematic change in dominant bacteria morphologies
361 during the biodegradation experiments. Note that the total cell number in surface waters of
362 Bolshezemelskaya Tundra were similar to those obtained in incubation experiments (see Table
363 1, Fig. S3).

364

365 3.2. Photodegradation of DOM from frozen peatlands

366 The pH of sunlight-exposed samples did not exhibit any systematic variation within 0.5
367 pH unit. The DIC remained fairly stable (within 0.5 mg/L) without any significant ($R^2 < 0.5$; $p >$
368 0.05) change during incubation, regardless of the type of system, DOC and DIC concentration
369 (not shown). The exposed water remained oxygenated (average O_2 saturation close to 90%) with
370 no detectable change (i.e. $> 10\%$) over the course of experiment. Specific conductivity also
371 remained highly stable over full period of exposure.

372 The bacteria count in photo-degradation reactors at the beginning of exposure and after
373 14 and 28 days of incubation yielded between 1 and 100 CFU mL^{-1} . This is a factor of 100 to
374 1000 lower than the number of cells in experiments of bio-degradation run in non-sterilized
375 waters over the same duration of experiments (section 3.1). As such, the microbial degradation
376 was considered negligible at our experimental conditions.

377 There was no sizeable decrease in DOC concentration during 28 d of exposure to sunlight
378 (Fig. 3 A). This relative change of DOC concentration ranged from -5 % to +5 % and it did not
379 exceed the non-systematic variability among triplicates. Although the triplicate agreed within
380 less than 2 % (the symbol size in Fig. 3), the small change of DOC in peat depression was similar
381 in light experiment and dark control. The % PDOC (relative to starting solution) as a function of

382 exposure time over 28 days of experiment ranged from 0 to 5% in peatbog depression and 0 to
383 10% in thermokarst lake and permafrost spring (**Fig 3 B**).

384 The $SUVA_{254\text{ nm}}$ in photodegradation experiments decreased much stronger than the
385 DOC. The SUVA decrease relative to control was mostly pronounced in permafrost stream (**Fig.**
386 **4**). The optical properties of DOC demonstrated sizeable decrease of E_{365}/E_{470} ratio
387 corresponding to UV/vis absorbing functional groups (**Fig. S4 A**), which was consistent with
388 decreasing $SUVA_{254\text{ nm}}$ during sunlight exposure. The E_{254}/E_{436} ratio, corresponding to
389 autochthonous vs. terrestrial DOM, did not demonstrate any sizeable change over the course of
390 experiment (**Fig. S4 B**).

391 Most of major and trace elements did not show any significant (at $p < 0.05$) change in
392 concentration over the photodegradation experiments. Only a few nutrients (P, Fe, Zn, B) and
393 trace metals (Zn, Ti, V, Zr, Nb and Th) demonstrated a decrease in concentration. The decrease
394 of Fe was mostly pronounced in permafrost stream, and did not occur in permafrost depression
395 (**Fig. 5 A**) whereas total dissolved phosphorus systematically decreased, by 20 to 50%, over 28
396 days of sunlight exposure in permafrost depression, thermokarst lake and permafrost stream (**Fig.**
397 **5 B**). A decrease of Ti, Zn, Nb and Th also occurred in thermokarst lake and permafrost stream
398 (not shown). Overall, the magnitude of decrease of P, Fe, Ti, V and Zn in photodegradation
399 experiments followed the order “permafrost stream > thermokarst lake > permafrost depression”.

400

401

402 **4. Discussion**

403 *4.1. High stability of dissolved organic matter to bio degradation in surface waters from*
404 *frozen peatland*

405 The unexpected result of this study was very low BDOC fraction, measured not only in
406 large river (Pechora) but also in small stream, thermokarst lake and peatland depressions formed

407 due to permafrost subsidence. According to compilation of available biodegradation studies, the
408 BDOC fraction (28 days) ranges from 3 to 18% (mean 13%) in waters of continuous permafrost
409 zone and from 5 to 15% (mean 14%) in discontinuous permafrost zone (Vonk et al., 2015). This
410 is higher than the 0 to 10 % of BDOC measured for all water objects from the discontinuous
411 permafrost zone in this study. Note that very few biodegradability studies in aquatic systems
412 dealt with frozen peatlands, and all previous incubation experiments used water from
413 mountainous regions on mineral soils and rocks in Scandinavia, Alaskan slope and Canada,
414 yedoma regions of Eastern Siberia, or the Yenisey basin. Only one former biodegradation study
415 in peat mire context demonstrated sizable bioavailability of soil aquatic leachate to lake water
416 bacteria (Roehm et al., 2009), but this work did not deal with pure aquatic endmember, unlike
417 this study. Instead, the BDOC of frozen peatlands surface waters measured for the
418 Bolshezemelskaya Tundra inland waters was comparable with the value suggested by Vonk et al
419 (2015) for non-permafrost aquatic DOC (0-1 %).

420 Another important point revealed in previous work on biodegradation of Arctic waters is
421 that aquatic BDOC in large streams and rivers decreased as the Arctic summer progressed (Vonk
422 et al., 2015), although this pattern was absent for **soil leachates** and small streams. In our case,
423 thermokarst lake Isino and r. Pechora can be considered as sufficiently large hydrological
424 systems. The sampling was performed in the end of July which is already summer baseflow
425 period and as such 0 to 5 % biodegradable DOC measured for Isino and Pechora in this study is
426 comparable with 0 to 20% BDOC loss reported in large streams and rivers at ~200 Julian day
427 (Vonk et al., 2015). However, small stream and permafrost subsidence remain clearly at the very
428 low edge of BDOC % lost reported for soils and streams in summer. In the estuarine zone of
429 largest European Arctic permafrost-free river, Severnaya Dvina, there was no measurable
430 biodegradation in spring, when the DOM was dominated by allochthonous sources, but a 15 to
431 20% decrease of DOC occurred during first 300 h in river water collected in August, when

432 sizeable phytoplankton productivity was observed (Shirokova et al., 2017b). In laboratory
433 experiments with individual cultures, moss and peat leachates were also sizably biodegraded over
434 1-2 days of exposure (Shirokova et al., 2017a), whereas the same bacterial species were not
435 capable degrading DOM from surface waters draining peatland and moss covered bogs
436 (Oleinikova et al., 2018). It is possible that in natural settings, the input of biolabile DOC from
437 terrestrial vegetation may enhance the bioavailability of stable DOC (e.g., Textor et al., 2018)
438 although this effect could not be tested in this study.

439 Mechanistic reasons for extremely low bioavailability of DOC from studied peatlands
440 remain unclear and require in-depth analysis of DOM molecular structure and stoichiometry as
441 well as high resolution microbial approaches. It is known that the DOM released from frozen
442 soils contains high proportions of biologically labile protein-like and photochemically reactive
443 aromatic substances (Gao et al., 2018). Following the pioneering study of Ward et al. (2017),
444 we hypothesize that, similar to DOC from organic (non-permafrost) layer, the concentration of
445 high-lability, aliphatic-like DOC in surface waters of frozen peatlands is too low to sustain
446 microbial population, or that this aquatic DOC, remaining after microbial processing of soil
447 porewater DOC is of low lability for microbes capable to degrade aliphatic-like DOC and
448 inhabiting aerobic zone of permafrost surface waters. The constant pattern of UV₂₅₄ absorbency
449 in biodegradation experiment was consistent with negligible change in BDOC over 28 days of
450 incubation. In comparison, the biodegradation of peat water from European boreal zone was
451 associated with an increase in SUVA by up to 7.4 %, which also implies an increase in the
452 proportion of aromatic compounds (Hulatt et al., 2014). The total bacterial number in studied
453 surface waters $(0.5-5) \times 10^6$ cell mL⁻¹ is in excellent agreement with other studies of thermokarst
454 peatland lake waters (Deshpande et al., 2016). Following these researchers, we suggest that the
455 reason of low biodegradability of peatland humic waters is that the majority of active bacteria
456 are associated with particles (> 3 µm) rather than present as free-living cells (< 1 µm) capable to

457 DOC processing. In addition, the bacterial communities are not just shaped by size fractionation
458 by filtration, but also the presence or absence of bacterial grazers (Dean et al., 2018). However,
459 further mechanistic studies of model aquatic bacterial communities capable to affect the
460 degradation of DOM from different terrestrial sources are necessary (Logue et al., 2016).

461 Interestingly, there was no measurable difference in BDOC at 4, 23 and 37°C, as the
462 proportion of BDOC at all temperatures for each system was below 5-10%. This result allows
463 preliminary prediction of possible consequence of climate change and surface water heating in
464 high latitudes. In a short-term climate warmings scenario, or assuming fast heating of surface
465 waters due to prolonged heat wave of draught occurring both in European, permafrost-free (see
466 Shirokova et al., 2013a) and western Siberian (Pokrovsky et al., 2013) permafrost-bearing
467 peatlands, we do not foresee any measurable change in biodegradability of DOM from the water
468 column. Under even most extreme heating scenario of thermokarst lakes, river and depressions
469 of the frozen peatland territories, the short-term bio-processing of aquatic DOM may remain
470 close to zero.

471
472 *4.2. Negligible impact of photodegradation on DOM transformation in inland waters of*
473 *frozen peatlands*

474 The second main result of this work was high stability of surface waters DOM to sunlight
475 exposure. Over 28 d of incubation in outdoor pools at the conditions corresponding to surface (<
476 0.05 m depth) water layer of thermokarst lakes and streams from permafrost zone, the change in
477 DOC concentration was less than 5-10% of the initial value and was not distinguishable from
478 that in the dark control (**Fig. 3 A, B**). Therefore, the DOM of all frozen peatland is quite refractory
479 and not subject to measurable photodegradation over 4 weeks of exposure. This period is
480 comparable with the water residence time in small depressions of frozen peatlands (Novikov et
481 al., 2009) and small thermokarst thaw ponds of frozen palsa peatbogs (Manasypov et al., 2015)

482 but much higher than the water travel time in small streams (< 10 km long) and in the lower
483 reaches of Pechora river, from the site of sampling till the Arctic Ocean (ca. several days). This
484 result apparently contradicts the recent paradigm that the photochemical oxidation may account
485 for 70 to 95% of total DOC processed in the water column of arctic lakes, rivers and soils (Cory
486 et al., 2013, 2014; Ward and Cory, 2016; Ward et al., 2017). However, the conclusion of this
487 group of authors is based on study of distilled water leachates of mineral soils, headwater streams,
488 fresh permafrost thaw sites and lakes of N. Alaska slopes, developed on mineral substrates. In
489 contrast, the results of DOM photolysis in polygonal and runnel ponds located in frozen peatlands
490 (2 m peat, 40-60 cm active layer thickness) of continuous permafrost regions (Canada High
491 Arctic) demonstrated a relatively fast decay of color and fluorescence, but insignificant losses of
492 DOC over 12 days of exposure time (Laurion and Mladenov, 2013). Recently, no measurable
493 photochemical loss of ancient permafrost DOC has been revealed in the thawing yedoma
494 permafrost sites of the Kolyma River, its tributaries and streams (Stubbins et al., 2017). Another
495 recent study of DOM photodegradation in boreal high-latitude peatland streams of the White Sea
496 watershed demonstrated only 10% decrease in DOC concentration over 10 days of incubation
497 under sunlight (Oleinikova et al., 2017). In the estuarine zone of the largest European Arctic river
498 draining wetland- and forest-dominated permafrost-free territory (Severnaya Dvina), we did not
499 find any measurable photo-degradation of DOM over 1 month of exposure (Chupakova et al.,
500 2018). This comparison clearly demonstrate highly contrasting DOM photolability between the
501 aquatic systems of N. America, draining through mineral soil substrates, and that of boreal and
502 subarctic peatlands.

503 Further, due to high homogeneity of organic substrate surrounding studied waters and
504 similar allochthonous origin of DOM in all surface waters of frozen peatlands, there was no
505 dramatic difference in DOM photodegradability over the hydrological continuum in NE
506 European Arctic, which also contrasts the results obtained in aquatic systems on mineral soils

507 (Cory et al., 2007, 2013; Reader et al., 2014). It is possible that either 1) photochemical
508 degradation of humic peat waters occurs very fast, during first **hours** to days upon their exposure
509 to sunlight or 2) that the nature of DOM is so refractory that much longer exposure periods, on
510 the order of several months to years (as in the Arctic coast) are necessary to photodegrade the
511 DOM from frozen peatlands. The first explanation is consistent with recent experiments on
512 photodegradation of fresh peat mire water, collected in taiga region of NW Russia, where about
513 50% of bogwater DOC was photodegraded over 2 days of exposure to sunlight (Oleinikova et
514 al., 2017).

515 As such, it is possible that all surface waters sampled for experiments in this study,
516 including stagnant water in permafrost depression, **have already contacted** with sunlight for more
517 than several days and thus became photo-resistant. Assuming the maximal possible DOC loss
518 due to photolysis assessed in our experiments ($0.1 \text{ mg C L}^{-1} \text{ d}^{-1}$ corresponding to a loss of 3 mg/L
519 during 28 days) and the light penetration depth of 0.5 m which is comparable with the typical
520 depth of studied water bodies, the photodegradation can **contribute to** less than 10 % of total CO_2
521 emission flux from the water surfaces of frozen peatlands ($0.4\text{-}0.8 \text{ g C m}^{-2} \text{ d}^{-1}$ in this work; 0.8
522 to $4.4 \text{ g C m}^{-2} \text{ d}^{-1}$ in western Siberian rivers and streams, located on very similar context of frozen
523 peat bogs, Serikova et al., 2018). The maximal PDOC value measured in this work is also at the
524 lower end range of DOM photodegradation contribution to C flux in North European boreal and
525 subarctic settings. Thus, DIC annual photo-production contributed between **1 and 8** % of CO_2
526 emissions from a humic lake in south of Sweden (Groeneveld et al., 2016) and globally in the
527 boreal and subarctic zone, sunlight-induced CO_2 emissions represent about one tenth to the CO_2
528 emission from lakes and reservoirs (Koehler et al., 2014).

529 The evolution of optical properties of DOM as a function of exposure time in different
530 samples **was** consistent with the mechanisms of photo-sensitive DOM removal during irradiation.
531 The ratio E_{365}/E_{470} is known to correlate with the degree of condensation of DOM aromatic

532 groups and with the degree of humification (Chin et al., 1994; Hur et al., 2006) whereas UV_{254}
533 is used as proxy for aromatic C and source of DOM (Chen et al., 1977; Uyguner and Bekbolet,
534 2005). The optical properties of DOC were much less conservative under sunlight exposure
535 compared to total dissolved C concentration, as $UV_{254\text{ nm}}$ and E_{365}/E_{470} ratio sizably decreased in
536 the course of experiments. Numerous studies of allochthonous riverine DOM also revealed that
537 photodegradation of colored DOM (CDOM) and $SUVA_{254}$ were much greater than DOC losses
538 (Spencer et al., 2009; Reche et al., 2000; Vähätalo and Wetzel, 2004; Mostofa et al., 2011; Bittar
539 et al., 2015; Gareis and Lesack, 2018). A decrease of E_{365}/E_{470} corresponded to removal of UV
540 rather than visual light absorbing functional groups, whereas a constant pattern of E_{254}/E_{436} ratio
541 **within** the hydrological continuum ‘depression → stream → lake → river’ was consistent with
542 lack of autochthonous DOM in all studied water objects, which were dominated by terrestrial
543 (aromatic) DOM from peat horizons. Overall, our observations confirm the conclusion achieved
544 from a recent compilation of available data across the world that degradation processes act
545 preferentially on CDOM rather than DOC concentration (Massicotte et al., 2017; Oleinikova et
546 al., 2017).

547 In contrast to DOC, sizeable removal of dissolved P and Fe together with some related
548 trace elements (Ti, V, Zn, Nb) during photolysis of surface waters reflects transformation and
549 coagulation of Fe-rich colloids, that behave independent on organic colloids in humic waters
550 (Vasyukova et al., 2010; Pokrovsky et al., 2016). This precipitation of Fe hydroxides together
551 with P and insoluble trace elements was mostly pronounced in permafrost stream which had the
552 **highest pH. In this stream, Fe(III) hydroxide was not stable due to pronounced hydrolysis. After**
553 **photolytic removal of small amount of DOM that stabilized colloidal Fe (Oleinikova et al., 2017),**
554 **Fe hydroxide could coagulate and coprecipitate P and some trace elements.**

555

556 4.3. *Lack of bio- and photodegradation in humic surface waters of frozen peat bogs*
557 *despite sizeable CO₂ emission*

558 The main fundamental result of the present study is that, despite well-known
559 supersaturation of lentic and lotic waters of frozen peatlands to atmospheric pCO₂, the surface
560 waters of frozen peatlands exhibit negligible bio- and photo-degradability over time scale (28
561 days) comparable with water residence time in various reservoirs. Although we lack seasonally
562 biased data set that therefore decreases the representability of results for the pan Arctic boreal
563 environment, our finding is at odds with the dominant paradigm that bio- and photodegradation
564 control the DOC removal from arctic aquatic ecosystems (Abbot et al., 2014; Cory et al., 2014;
565 Spencer et al., 2015). Given incontestable bio- and photodegradability of peat pore waters and
566 frozen soil extracts reported across the Arctic (Vonk et al., 2015; Selvam et al., 2017), this
567 strongly suggests that the DOM that arrives to small rivers and even permafrost depressions via
568 lateral peat soil outflux is already highly degraded. This is consistent with general idea that rates
569 of DOM photochemical alteration and rates of microbial responses to altered DOM are typically
570 rapid, from minutes to days (Cory and Kling, 2018). As such, the majority of elevated CO₂
571 measured in surface waters of permafrost peat landscape originates from degradation of soil
572 water DOM once it enters open surface water. This is especially true for photo-oxidation, which
573 is not likely to occur in the soil.

574 We believe that the degradation of soil DOM in surface waters of frozen peatlands occurs
575 very fast and completes within first hours or days. This is shorter than the residence time of water
576 in permafrost depressions, thaw ponds and rivers. As a result, we did not detect sizeable bio- and
577 photodegradation of residual DOM in various types of inland waters from permafrost landscapes.
578 In order to explain persistent CO₂ supersaturation of inland waters from peatlands, we suggest
579 that benthic respiration of stream, lake and river sediments produce sizeable amount of CO₂ thus
580 increasing overall C emission potential of the aquatic systems (MacIntyre et al., 2018; Valle et

581 al., 2018). For example, anaerobic C mineralization of thermokarst lake sediments is fairly well
582 established in discontinuous permafrost zone of peat bogs in western Siberia (Audry et al., 2011)
583 and Canada (Deshpande et al., 2017). Note that the potential for dark DOM chemical oxidation
584 in iron-rich organic-rich waters facing redox oscillation (i.e., Page et al., 2012) is rather low in
585 studied thermokarst waters which remain essentially oxic over full depth of the water column
586 during unfrozen period of the year.

587 The findings of this study and widely reported dominance of non-biodegradable DOC (0-
588 1% BDOC) in large rivers and streams of the non-permafrost zone (Vonk et al., 2015) suggest
589 that 1) the majority of BDOC is degraded before its arrival to large aquatic reservoirs, and 2) the
590 CO₂ supersaturation and emission of surface waters from frozen peatlands is due to soil pore
591 water and sediment respiration rather than aerobic bio- and photo-degradation of DOM in the
592 water column. Further, the non-increase in BDOC fraction during temperature rise from 4 to
593 37°C implies that, within the climate warming scenario, the heating of peat surface waters will
594 be a minor factor of overall CO₂ balance. Instead, the change of water path and residence time in
595 pore waters of frozen peatlands, the rate of supra-permafrost water delivery, and the magnitude
596 of benthic respiration in large rivers and thermokarst lakes may control the CO₂ emission from
597 inland waters.

598

599 **Conclusions**

600 This work revealed high resistance of surface waters collected in permafrost peatland to
601 both bio- and photo-degradation. Less than 5-10% of the initial aquatic DOC was removed over
602 1 month of dark aerobic incubation at 4, 22 and 37°C as well as during sunlight exposure of
603 sterile-filtered waters. In contrast to expected differences in bio- and photo-lability between small
604 permafrost subsidences, streams, large lake and the Pechora River, there was no measurable
605 difference in surface waters BDOC concentration along the hydrological continuum. The

606 contribution of aerobic DOM biodegradation within the water column to observed CO₂
607 supersaturations and net CO₂ emission fluxes from bog water, lakes, streams and rivers of
608 peatland territories located within discontinuous permafrost zone is less than 10%. Despite
609 decrease in CDOM during photolysis, this process does not significantly contribute to total DOC
610 degradation and C emission from the surface of inland waters of frozen peatlands.

611 We hypothesize that refractory nature of DOM from frozen peatlands which is already
612 processed in soil waters before arriving to lentic and lotic surface reservoirs create unfavorable
613 conditions for biodegradation. The reason for high stability of DOM from frozen peatland to
614 photolysis is less clear but can be linked to fast photo-degradation of peat bog and soil shallow
615 underground) waters after their exposure to the surface, occurring within the first hours to days.
616 We conclude on negligible impact of bio- and photo-degradation on DOM processing and CO₂
617 emission in surface waters of frozen peatlands. **This may require revisiting the current paradigm**
618 **of the importance of bio- and photo-degradation of DOC for CO₂ emission in permafrost**
619 **peatlands and clearly calls** for future work to quantify bio- and photo-lability of peat pore waters,
620 thawing soil ice, and suprapermfrost flow, which deliver the DOM to the rivers, lakes and
621 depressions.

622

623 **Acknowledgements**

624 This work was supported by RFFI (RFBR) grants No 17-05-00348_a and 17-05-00342_a,
625 Program FANO No 0409-2015-0140, RFFI No 18-05-01041 and UroRAN No 18-9-5-29.
626 Additional funding from JPI Climate initiative, financially supported by VR (the Swedish
627 Research Council) grant no. 325-2014-6898, is also acknowledged.

628

629 **References**

630 Abbott, B. W., Larouche, J. R., Jones, J. B., Bowden, W. B., and Balsler, A. W.: Elevated
631 dissolved organic carbon biodegradability from thawing and collapsing permafrost, J.
632 Geophys. Res., 119, 2049–2063, 2014.

633 Amado, A. M., Cotner, J. B., Cory, R. M., Edhlund, B. L., and McNeill, K.: Disentangling the
634 interactions between photochemical and bacterial degradation of dissolved organic matter:
635 amino acids play a central role, *Microb. Ecol.*, 69(3), 554-566, 2014.

636 Andersson, M. G. I., Catalán, N., Rahman, Z., Tranvik, L. J., and Lindström, E. S.: Effects of
637 sterilization on dissolved organic carbon (DOC) composition and bacterial utilization of
638 DOC from lakes, *Aquat. Microb. Ecol.*, 82, 199-208, 2018.

639 Ask, J., Karlsson, J., and Jansson, M.: Net ecosystem production in clear-water and brown-water
640 lakes, *Glob. Biogeochem. Cycles*, 26, GB1017, doi:10.1029/2010GB003951, 2012.

641 Audry, S., Pokrovsky, O. S., Shirokova, L. S., Kirpotin, S. N., and Dupré, B.: Organic matter
642 mineralization and trace element post-depositional redistribution in Western Siberia
643 thermokarst lake sediments, *Biogeosciences*, 8, 3341-3358, 2011.

644 Berggren, M., Laudon, H., Haei, M., Ström, L., and Jansson, M.: Efficient aquatic bacterial
645 metabolism of dissolved low-molecular-weight compounds from terrestrial sources, *ISME*
646 *J.*, 4, 408-416, 2010.

647 Bittar, T. B., Vieira, A. A. H., Stubbins, A., and Mopper, K.: Competition between
648 photochemical and biological degradation of dissolved organic matter from the
649 cyanobacteria *Microcystis aeruginosa*, *Limnol. Oceanogr.*, 60, 1172-1194, 2015.

650 Brittain, J. F., Gislason, G. M., Ponomarev, V. I., Bogen, J., Jensen, A. J., Khokhlova, L. G.,
651 Kochanov, S. K., Kokovkin, A. V., Melvold, K., Olafsson, J. S., Pettersson, L.-E., and
652 Stenina, A. S.: Arctic Rivers (chapter 9), pp. 337-379. In: *Rivers of Europe*, Eds: Tockner
653 K., Uehlinger U., Robinson C.T., Academic Press Elsevier, 2009.

654 Chen, Y., Senesi, N., and Schnitzer, M.: Information provided on humic substances by E4/E6
655 ratios, *Soil Sci. Soc. Amer. J.*, 41, 352-358, 1977.

656 Chin, Y.-P., Aiken, G., and O'Loughlin, E.: Molecular weight, polydispersity, and spectroscopic
657 properties of aquatic humic substances. *Environ. Sci. Technol.*, 28, 1853-1858, 1994.

658 Chupakova, A. A., Chupakov, A. V., Neverova, N. V., Shirokova, L. S., and Pokrovsky, O. S.:
659 Photodegradation of river dissolved organic matter and trace metals in the largest European
660 Arctic estuary. *Sci. Total Environ.*, 622–623, 1343–1352, 2018.

661 Cole, J. J. and Caraco, N. : Atmospheric exchange of carbon dioxide in a low-wind oligotrophic
662 lake measured by the addition of SF6. *Limnol. Oceanogr.*, 43, 647–656, 1998.

663 Cory, R. M., McKnight, D., Chin, Y. P., Miller, P., and Jaros, C. L.: Chemical characteristics of
664 fulvic acids from Arctic surface waters: Microbial contributions and photochemical
665 transformations, *J. Geophys. Res.*, 112, G04S51, doi:10.1029/2006JG000343, 2007.

666 Cory, R. M., Crump, B. C., Dobkowski, J. A., and Kling, G. W.: Surface exposure to sunlight
667 stimulates CO₂ release from permafrost soil carbon in the Arctic, *Proc. Natl. Acad. Sci. USA*,
668 110(9), 3429-3434, 2013.

669 Cory, R. M., Ward, C. P., Crump, B. C., and Kling, G. W.: Sunlight controls water column
670 processing of carbon in arctic fresh waters, *Science*, 345, 925-928, 2014.

671 Cory, R. M., Harrold, K. H., Neilson, B. T., Kling, G. W.: Controls on dissolved organic matter
672 (DOM) degradation in a headwater stream: the influence of photochemical and hydrological
673 conditions in determining light-limitation or substrate-limitation of photo-degradation,
674 *Biogeosciences*, 12, 6669–6685, 2015.

675 Cory, R. M., Kling, G. W.: Interactions between sunlight and microorganisms influence
676 dissolved organic matter degradation along the aquatic continuum, *Limnol. Oceanogr. Lett.*,
677 3, 102–116, 2018.

678 Dean, J. F., van Hal, J. R., Dolman, A. J., Aerts, R., and Weedon, J. T.: Filtration artefacts in
679 bacterial community composition can affect the outcome of dissolved organic matter

680 biolability assays, *Biogeosciences*, 15, 7141-7154, [https://doi.org/10.5194/bg-15-7141-](https://doi.org/10.5194/bg-15-7141-2018)
681 2018, 2018.

682 Dean, J. F., Garnett, M. H., Spyrakos, E., Billett, M. F.: The potential hidden age of dissolved
683 organic carbon exported by peatland streams, *J. Geophys. Res.: Biogeosciences*,
684 124, 328–341, 2019.

685 Deshpande, B. N., Maps, F., Matveev, A., and Vincent, W. F., 2017. Oxygen depletion in
686 subarctic peatland thaw lakes, *Arctic Science*, 3(2), 406-428, 2017.

687 Deshpande, B. N., Crevecoeur, S., Matveev, A., and Vincent, W. F.: Bacterial production in
688 subarctic peatland lakes enriched by thawing permafrost, *Biogeosciences*, 13, 4411-4427,
689 2016.

690 Drake, T. W., Holmes, R. M., Zhulidov, A. V., Gurtovaya, T., Raymond, P. A., McClelland, J.
691 W., and Spencer, R. G. M.: Multidecadal climate-induced changes in Arctic tundra lake
692 geochemistry and geomorphology, *Limnol. Oceanogr.*, 64, S179-S191, 2019.

693 Gao, L., Zhou, Z., Reyes, A. V., and Guo, L.: Yields and characterization of dissolved organic
694 matter from different aged soils in northern Alaska, *J. Geophys. Res.: Biogeosciences*, 123,
695 2035–2052, 2018.

696 Gareis, J. A. L., and Lesack, L. F. W.: Photodegraded dissolved organic matter from peak freshet
697 river discharge as a substrate for bacterial production in a lake-rich great Arctic delta, *Arctic*
698 *Science*, 4(4), 557-583, 2018.

699 Groeneveld, M., Tranvik, L., Natchimuthu, S., and Koehler, B.: Photochemical mineralisation in
700 a boreal brown water lake: considerable temporal variability and minor contribution to
701 carbon dioxide production, *Biogeoscience*, 13, 3931-3943, 2016.

702 Helms, J. R., Stubbins, A., Ritchie, J. D., Minor, E. C., Kieber, D. J., Mopper, K.: Absorption
703 spectral slopes and slope ratios as indicators of molecular weight, source, and
704 photobleaching of chromophoric dissolved organic matter, *Limnol. Oceanogr.*, 53(3), 955-
705 969, 2008.

706 Holmes, R. M., McClelland, J. W., Raymond, P. A., Frazer, B. B., Peterson, B. J., and Stieglitz, M.:
707 Labiality of DOC transported by Alaskan rivers to the Arctic Ocean, *Geophys. Res. Lett.*, 35,
708 L03402, doi:10.1029/2007GL032837, 2008.

709 Hulatt, C. J., Kaartokallio, H., Asmala, E., Autio, R., Stedmon, C. A., Sonninen, E., Oinonen,
710 M., and Thomas, D. N.: Bioavailability and radiocarbon age of fluvial dissolved organic
711 matter (DOM) from a northern peatland-dominated catchment: effect of land-use change,
712 *Aquat. Sci.*, 76(3), 393-404, 2014.

713 Hur, J., Williams, M. A., and Schlautman, M. A.: Evaluating spectroscopic and chromatographic
714 techniques to resolve dissolved organic matter via end member mixing analysis, *Chemosphere*,
715 63, 387-402, 2006.

716 Ilina, S. M., Drozdova, O. Yu., Lapitsky, S. A., Alekhin, Yu. V., Demin, V. V., Zavgorodnaya, Yu.
717 A., Shirokova, L. S., Viers, J., and Pokrovsky, O. S.: Size fractionation and optical properties
718 of dissolved organic matter in the continuum soil solution-bog-river and terminal lake of a
719 boreal watershed, *Org. Geochem.*, 66, 14–24, 2014.

720 Kaiser, K., Canedo-Oropeza, M., McMahon, R., and Amon, R. M. W.: Origins and
721 transformations of dissolved organic matter in large Arctic rivers, *Sci. Reports*, 7, 13064,
722 2017.

723 Karlsson, J., Jansson, M., and Jonsson, A.: Respiration of allochthonous organic carbon in
724 unproductive forest lakes determined by the Keeling plot method, *Limnol. Oceanogr.*, 52,
725 603-608, 2007.

726 Koehler, B., Landelius, T., Weyhenmeyer, G. A., Machida, N., and Tranvik, L.J.: Sunlight-
727 induced carbon dioxide emissions from inland waters, *Global Biogeochem. Cycles*, 28, 696–
728 711, 2014.

- 729 Köhler, S., Buffam, I., Jonsson, A., and Bishop, K.: Photochemical and microbial processing of
730 stream and soil water dissolved organic matter in a boreal forested catchment in northern
731 Sweden, *Aquat. Sci.*, 64, 269–281, 2002.
- 732 Lapiere, J.-F., Guillemette, F., Berggren, M., and del Giorgio, P. A.: Increases in terrestrially
733 derived carbon stimulate organic carbon processing and CO₂ emissions in boreal aquatic
734 ecosystems, *Nature Comm.*, 4, 2972, doi:10.1038/ncomms3972, 2013.
- 735 Larouche, J. R., Abbott, B. W., Bowden, W. B., Jones, and J. B.: The role of watershed
736 characteristics, permafrost thaw, and wildfire on dissolved organic carbon biodegradability
737 and water chemistry in Arctic headwater streams, *Biogeosciences*, 12, 4221–4233, 2015.
- 738 Laurion, I., and Mladenov, N.: Dissolved organic matter photolysis in Canadian Arctic thaw
739 ponds, *Environ. Res. Lett.*, 8, 035026, doi.org/10.1088/1748-9326/8/3/035026, 2013.
- 740 Logue, J. B., Stedmon, C. A., Kellerman, A. M., Nielsen, N. J., Andersson, A. F., Laudon, H.,
741 Lindström, E. S., and Kritzberg, E. S.: Experimental insights into the importance of aquatic
742 bacterial community composition to the degradation of dissolved organic matter, *ISME J.*,
743 10, 533–545, 2016.
- 744 Lou, T., and Xie, H.: Photochemical alteration of the molecular weight of dissolved organic
745 matter, *Chemosphere*, 65, 2333–2342, 2006.
- 746 MacIntyre, S., Cortes, A., and Sadro, S.: Sediment respiration drives circulation and production
747 of CO₂ in ice-covered Alaskan arctic lakes, *Limnol. Oceanogr. Lett.*, 3, 302–310, 2018.
- 748 Manasyrov, R. M., Pokrovsky, O. S., Kirpotin, S. N., Shirokova, L. S.: Thermokarst lake waters
749 across permafrost zones of Western Siberia, *Cryosphere* 8, 1177–1193, 2014.
- 750 Manasyrov, R. M., Vorobyev, S. N., Loiko, S. V., Kritzkov, I. V., Shirokova, L. S., Shevchenko,
751 V. P., Kirpotin, S. N., Kulizhsky, S. P., Kolesnichenko, L. G., Zemtsov, V. A., Sinkinov, V.
752 V., and Pokrovsky, O. S.: Seasonal dynamics of organic carbon and metals in thermokarst
753 lakes from the discontinuous permafrost zone of western Siberia, *Biogeosciences*, 12, 3009–
754 3028, 2015.
- 755 Mann, P. J., Davydova, A., Zimov, N., Spencer, R. G. M., Davydov, S., Bulygina, E., Zimov, S.,
756 Holmes, R. M.: Controls on the composition and lability of dissolved organic matter in
757 Siberia’s Kolyma River basin, *J. Geophys. Res.*, 117, G01028, doi: 10.1029/2011JG001798,
758 2012.
- 759 Mann, P. J., Sobczak, W. V., LaRue, M. M., Bulygina, E., Davydova, A., Vonk, J. E., Schade,
760 J., Davydov, S., Zimov, N., Holmes, R. M., Spencer, R. G. M.: Evidence for key enzymatic
761 controls on metabolism of Arctic river organic matter, *Global Change Biol.*, 20(4), 1089–
762 1100, 2014.
- 763 Mann, P. J., Eglinton, T. I., Mcintyre, C. P., Zimov, N., Davydova, A., Vonk, J. E., Holmes, R.
764 M., Spencer, R. G. M.: Utilization of ancient permafrost carbon in headwaters of Arctic
765 fluvial networks, *Nat. Commun.*, 6, doi: 10.1038/ncomms8856, 2015.
- 766 Massicotte, P., Asmala, E., Stedmon, C., Markager, S.: Global distribution of dissolved matter
767 along the aquatic continuum: Across rivers, lakes and oceans, *Sci. Total Environ.*, 609, 180–
768 191, 2017.
- 769 McCallister, S. L., and del Giorgio, P. A.: Direct measurement of the $\delta^{13}\text{C}$ signature of carbon
770 respired by bacteria in lakes: Linkages to potential carbon sources, ecosystem baseline
771 metabolism, and CO₂ fluxes, *Limnol. Oceanogr.*, 53(4), 1204–1216, 2008.
- 772 **Moody, C. S., Worrall, F., Evans, C. D., Jones, T. G.: The rate of loss of dissolved organic carbon**
773 **(DOC) through a catchment, *J. Hydrol.*, 492, 139–150, 2013.**
- 774 Moran, M. A., Sheldon, W. M., and Zepp, R. G.: Carbon loss and optical property changes during
775 long-term photochemical and biological degradation of estuarine dissolved organic matter,
776 *Limnol. Oceanogr.*, 45, 1254–1264, 2000.

777 Mostofa, K. M. G., Yoshioka, T., Konohira, E., and Tanoue, E.: Photodegradation of fluorescent
778 dissolved organic matter in river waters, *Geochem. J.*, 41, 323-331, 2007.

779 Mostofa, K. M. G., Wu, F., Liu, C-Q., Vione, D., Yoshioka, T., Sakugawa, H., and Tanoue, E.:
780 Photochemical, microbial and metal complexation behavior of fluorescent dissolved organic
781 matter in the aquatic environments, *Geochem. J.*, 45, 235-254, 2011.

782 Novikov, S. M., Moskvina, Y. P., Trofimov, S. A., Usova, L. I., Batuev, V. I., Tumanovskaya, S. M.,
783 Smirnova, V. P., Markov, M. L., Korotkevich, A. E., and Potapova, T. M.: Hydrology of bog
784 territories of the permafrost zone of western Siberia, *BBM publ. House, St. Petersburg*, 535
785 pp. (in Russian), 2009.

786 Oleinikova, O., Drozdova, O. Y., Lapitskiy, S. A., Bychkov, A. Y., and Pokrovsky, O. S.:
787 Dissolved organic matter degradation by sunlight coagulates organo-mineral colloids and
788 produces low-molecular weight fraction of metals in boreal humic waters, *Geochim.
789 Cosmochim. Acta*, 211, 97-114, 2017.

790 Oleinikova, O., Shirokova, L. S., Drozdova, O. Y., Lapitskiy, S. A., and Pokrovsky, O. S.: Low
791 biodegradability of dissolved organic matter and trace metal from subarctic waters by culturable
792 heterotrophic bacteria, *Sci. Total Environ.*, 618, 174-187, 2018.

793 Page, S. E., Sander, M., Arnold, W. A., and McNeill, K.: Hydroxyl radical formation upon
794 oxidation of reduced humic acids by oxygen in the dark, *Environ. Sci. Technol.*, 46, 1590-
795 1597, 2012.

796 Peacock, M., Evans, C. D., Fenner, N., Freeman, C., Gough, R., Jones, T. G., and Lebron, I.:
797 UV-visible absorbance spectroscopy as a proxy for peatland dissolved organic carbon
798 (DOC) quantity and quality: considerations on wavelength and absorbance degradation,
799 *Environmental Science: Processes and Impacts*, 10–12, doi:10.1039/c4em00108g, 2014

800 Pickard, A. E., Heal, K. V., McLeod, A. R., and Dinsmore, K. J.: Temporal changes in
801 photoreactivity of dissolved organic carbon and implications for aquatic carbon fluxes from
802 peatlands, *Biogeosciences*, 14, 1793-1809, <https://doi.org/10.5194/bg-14-1793-2017>, 2017.

803 Pokrovsky, O. S., Shirokova, L. S., Zabelina, S. A., Vorobieva, T. Ya., Moreva, O. Yu., Klimov,
804 S. I., Chupakov, A. V., Shorina, N. V., Kokryatskaya, N. M., Audry, S., Viers, J., Zoutien,
805 C., and Freydisier, R.: Size fractionation of trace elements in a seasonally stratified boreal
806 lakes: Control of organic matter and iron colloids, *Aquat. Geochem.*, 18, 115–139, 2012.

807 Pokrovsky, O. S., Shirokova, L. S., Kirpotin, S. N., Kulizhsky, S. P., Vorobiev, S. N.: Impact of
808 Western Siberia heat wave 2012 on greenhouse gases and trace metal concentration in thaw
809 lakes of discontinuous permafrost zone, *Biogeosciences*, 10, 5349–5365, 2013.

810 Pokrovsky, O. S., Manasypov, R. M., Shirokova, L. S., Loiko, S. V., Krickov, I. V., Kopysov,
811 S., and Kirpotin, S. N.: Permafrost coverage, watershed area and season control of dissolved
812 carbon and major elements in western Siberia rivers, *Biogeosciences*, 12, 6301–6320, 2015.

813 Pokrovsky, O. S., Manasypov, R. M., Loiko, S. V., and Shirokova, L. S.: Organic and organo-
814 mineral colloids of discontinuous permafrost zone, *Geochim. Cosmochim. Acta*, 188, 1–20,
815 2016.

816 Porcal, P., Dillon, P. J., and Molot, L. A.: Photochemical production and decomposition of
817 particulate organic carbon in a freshwater stream, *Aquat. Sci.*, 75, 469–482, 2013.

818 Porcal, P., Dillon, P. J., and Molot, L. A.: Interaction of extrinsic chemical factors affecting
819 photodegradation of dissolved organic matter in aquatic ecosystems, *Photochem. Photobiol.
820 Sci.*, 13, 799-812, 2014.

821 Porcal, P., Dillon, P. J., and Molot, L. A.: Temperature dependence of photodegradation of
822 dissolved organic matter to dissolved inorganic carbon and particulate organic carbon, *Plos
823 ONE*, 10(6), e0128884, DOI:10.1371/journal.pone.0128884, 2015.

824 Porter, K. G., and Feig, Y. S.: The use of DAPI for identifying and counting aquatic microflora,
825 *Limnol. Oceanogr.*, 25: 943–948, 1980.

826 Raudina, T. V., Loiko, S. V., Lim, A., Manasyov, R. M., Shirokova, L. S., Istigecev, G. I.,
827 Kuzmina, D. M., Kulizhsky, S. P., Vorobyev, S. N., and Pokrovsky, O. S.: Permafrost thaw
828 and climate warming may decrease the CO₂, carbon, and metal concentration in peat soil
829 waters of the Western Siberia Lowland, *Sci. Total Environ.*, 634, 1004-1023, 2018.

830 Reader, H. E., Stedmon, C. A., and Kritzberg, E. S.: Seasonal contribution of terrestrial organic
831 matter and biological oxygen demand to the Baltic Sea from three contrasting river
832 catchments, *Biogeosciences* 11, 3409-3419, 2014.

833 Reche, I., Pace, M. L., and Cole, J. J.: Modeled effects of dissolved organic carbon and solar
834 spectra on photobleaching in lake ecosystems, *Ecosystems* 3, 419-432, 2000.

835 Roehm, C. L., Giesler, R., Karlsson, J.: Bioavailability of terrestrial organic carbon to lake
836 bacteria: The case of a degrading subarctic permafrost mire complex, *J. Geophys. Res.*, 114,
837 G03006, doi: 10.1029/2008JG000863, 2009.

838 Selvam, B. P., Lapierre, J.-F., Guillemette, F., Voigt, C., Lamprecht, R. E., Biasi, C., Christensen,
839 T. R., Martikainen P. J., and Berggren, M.: Degradation potentials of dissolved organic
840 carbon (DOC) from thawed permafrost peat. *Scientific Reports*, 7, Art No 45811, doi:
841 10.1038/srep45811, 2016.

842 Serikova, S., Pokrovsky, O. S., Ala-aho, P., Kazantsev, V., Kirpotin, S. N. Kopysov, S. G.,
843 Krickov, I. V., Laudon, H., Manasyov, R. M., Shirokova, L. S., Sousby, C., Tetzlaff, D.,
844 Karlsson, J.: High riverine CO₂ emissions at the permafrost boundary of Western Siberia.
845 *Nature Geoscience*, 11, 825-829, 2018.

846 Serikova S., Pokrovsky O. S., Laudon, H., Krickov, I. V., Lim, A. G., Manasyov, R. M.,
847 Karlsson, J.: C emissions from lakes across permafrost gradient of Western Siberia. *Nature*
848 *Comm.*, in press, 2019.

849 Shirokova, L. S., Pokrovsky, O. S., Moreva, O. Y., Chupakov, A. V., Zabelina, S. A., Klimov,
850 S. I., Shorina, N. V., and Vorobieva T. Y.: Decrease of concentration and colloidal fraction
851 of organic carbon and trace elements in response to the anomalously hot summer 2010 in a
852 humic boreal lake, *Sci. Tot. Environ.*, 463-464, 78–90, 2013a.

853 Shirokova, L. S., Pokrovsky, O. S., Kirpotin, S. N., Desmukh, C., Pokrovsky, B. G., Audry, S.,
854 and Viers, J.: Biogeochemistry of organic carbon, CO₂, CH₄, and trace elements in
855 thermokarst water bodies in discontinuous permafrost zones of Western Siberia,
856 *Biogeochemistry*, 113, 573–593, 2013b.

857 Shirokova, L. S., Bredoire, R., Rolls, J. L., and Pokrovsky, O. S.: Moss and peat leachate
858 degradability by heterotrophic bacteria: fate of organic carbon and trace metals,
859 *Geomicrobiol. J.*, 34(8), 641-655, 2017a.

860 Shirokova, L. S., Chupakova, A. A., Chupakov, A. V., and Pokrovsky, O.S.: Transformation of
861 dissolved organic matter and related trace elements in the mouth zone of the largest European
862 Arctic river: experimental modeling, *Inland Waters*, 7(3), 272-282, 2017b.

863 Spencer, R. G. M., Stubbins, A., Hernes, P. J., Baker, A., Mopper, K., Aufdenkampe, A. K.,
864 Dyda, R. Y., Mwamba, V. L., Mangangu, A. M., Wabakanghanzi, J. N., and Six, J.:
865 Photochemical degradation of dissolved organic matter and dissolved lignin phenols from
866 the Congo River, *J. Geophys. Res.*, 114, G03010, doi: 10.1029/2009JG000968, 2009.

867 Spencer, R. G. M., Mann, P. J., Dittmar, T., Eglinton, T. I., McIntyre, C., Holmes, R. M., Zimov,
868 N., Stubbins, A.: Detecting the signature of permafrost thaw in Arctic rivers, *Geophys. Res.*
869 *Lett.*, 42, 2830-2835, 2015.

870 Stubbins, A., Mann, P. J., Powers, L., Bittar, T. B., Dittmar, T., McIntyre, C. P., Eglinton, T. I.,
871 Zimov, N., and Spencer, R. G. M.: Low photolability of yedoma permafrost dissolved

872 organic carbon, *J. Geophys. Res. Biogeosci.*, 122, 200-211, doi: 10.1002/2016JG003688,
873 2017.

874 Stutter, M. I., Richards, S., and Dawson, J. J. C.: Biodegradability of natural dissolved organic
875 matter collected from a UK moorland stream, *Water Res.*, 47(3), 1169-1180, 2013.

876 Sulzberger, B., Austin, A. T., Cory, R. M., Zepp, R. G., and Paul, N. D.: Solar UV radiation in
877 a changing world: roles of cryosphere-land-water-atmosphere interfaces in global
878 biogeochemical cycles, *Photochem. Photobiol. Sci.*, doi: 10.1039/c8pp90063a, 2019.

879 Tarnocai, C., Canadell, J. G., E. Schuur A. G., Kuhry P., Mazhitova G., and Zimov S.: Soil
880 organic carbon pools in the northern circumpolar permafrost region, *Global Biogeochem.*
881 *Cy.*, 23, GB2023, <https://doi.org/10.1029/2008GB003327>, 2009.

882 Textor, S. R., Guillemette, F., Zito, P. A., Spencer, R. G. M.: An assessment of dissolved
883 organic carbon biodegradability and priming in blackwater systems, *J. Geophys. Res.*
884 *Biogeosciences*, 123(9), 2998-3015, 2018.

885 Uyguner, C., and Bekbolet, M. : Implementation of spectroscopic parameters for practical
886 monitoring of natural organic matter, *Desalination*, 176, 47-55, 2005.

887 Valle, J., Gonsior, M., Hairir, M., Enrich-Prast, A., Schmitt-Kopplin, P., Bastviken, D., Conrad
888 R., and Hertkorn, N.: Extensive processing of sediment pore water dissolved organic
889 matter during anoxic incubation as observed by high-field mass spectrometry (FTICR-
890 MS), *Water Research*, 129, 252-263, 2018.

891 Vähätalo, A. V., Salonen, K., Münster, U., Järvinen, M., and Wetzel, R. G.: Photochemical
892 transformation of allochthonous organic matter provides bioavailable nutrients in a humic
893 lake, *Acta Hydrobiol.*, 156, 287-314, 2003.

894 Vähätalo, A. V. and Wetzel, R.G.: Photochemical and microbial decomposition of chromophoric
895 dissolved organic matter during long (months-years) exposures, *Mar. Chem.*, 89, 313-326,
896 2004.

897 Vasyukova, E., Pokrovsky, O. S., Viers, J., Oliva, P., Dupré, B., Martin, F., and Candaudap, F.:
898 Trace elements in organic- and iron-rich surficial fluids of boreal zone: Assessing colloidal
899 forms via dialysis and ultrafiltration, *Geochim. Cosmochim. Acta*, 74, 449-468, 2010.

900 Vonk, J. E., Tank, S. E., Mann, P. J., Spencer, R. G. M., Treat, C. C., Striegl, R. G., Abbott,
901 B. W., and Wickland K. P.: Biodegradability of dissolved organic carbon in permafrost
902 soils and aquatic systems: a meta-analysis, *Biogeosciences*, 12, 6915-6930, 2015.

903 Ward, C. P., Cory, R. M.: Complete and partial photo-oxidation of dissolved organic matter
904 draining permafrost soils, *Environ. Sci. Technol.*, 50(7), 3545-3553, 2016.

905 Ward, C. P., Nalven, S. G., Crump, B. C., Kling, G. W., and Cory, R. M.: Photochemical
906 alteration of organic carbon draining permafrost soils shifts microbial metabolic pathways
907 and stimulates respiration, *Nature Comm.*, 8, Art No 772, 2017.

908 Wauthy M., Rautio, M., Christoffersen, K. S., Forsstrom, L., Laurion, I., Mariash, H. L., Peura,
909 S., Vincent, W. F.: Increasing dominance of terrigenous organic matter in circumpolar
910 freshwaters due to permafrost thaw, *Limnol. Oceanogr. Lett.*, 3, 2018, 186–198, 2012.

911 Weishaar, J. L., Aiken, G. R., Bergamaschi, B. A., Fram, M. S., Fujii, R., Mopper, K.:
912 Evaluation of specific ultraviolet absorbance as an indicator of the chemical composition
913 and reactivity of dissolved organic carbon, *Environ. Sci. Technol.*, 37, 4702–4708, 2003.

914 Wickland, K. P., Aiken G. R., Butler K., Dornblaser M. M., Spencer R. G. M., and Striegl R.
915 G.: Biodegradability of dissolved organic carbon in the Yukon River and its tributaries:
916 seasonality and importance of inorganic nitrogen. *Glob Biogeochem Cycle* 26,
917 2012gb004342, 2012.

918 Wilkinson, G. M., Pace, M. L., and Cole, J. J. : Terrestrial dominance of organic matter in north
919 temperate lakes, *Global. Biogeochem. Cycles* 27, 43-51, 2013.

920 Winter, A. R., Fish, T. A. E., Playle, R. C., Smith, D. S., and Curtis, P. J.: Photodegradation of
 921 natural organic matter from diverse freshwater sources, *Aquat. Toxicol.*, 84, 215-222,
 922 2007.

923

924

925

926

927

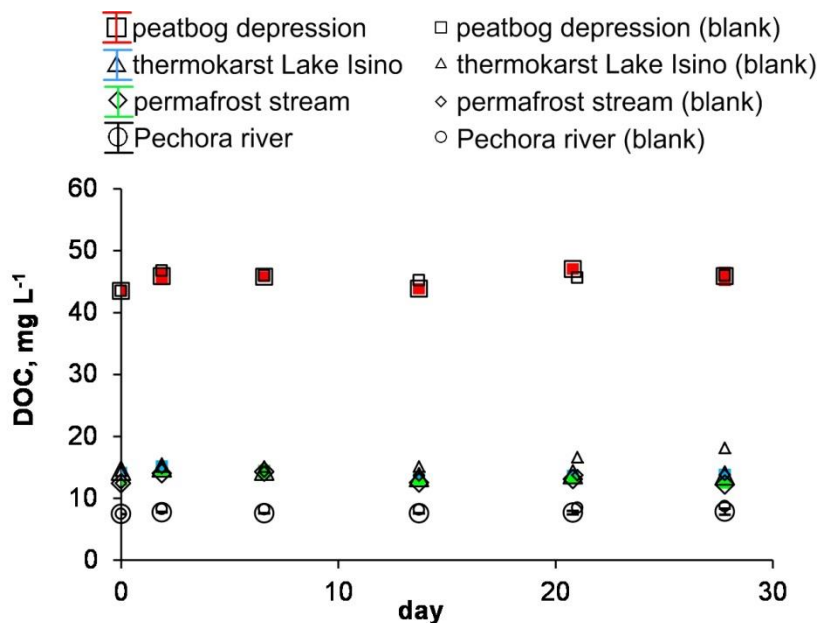
928

929

930

931

932



933

934

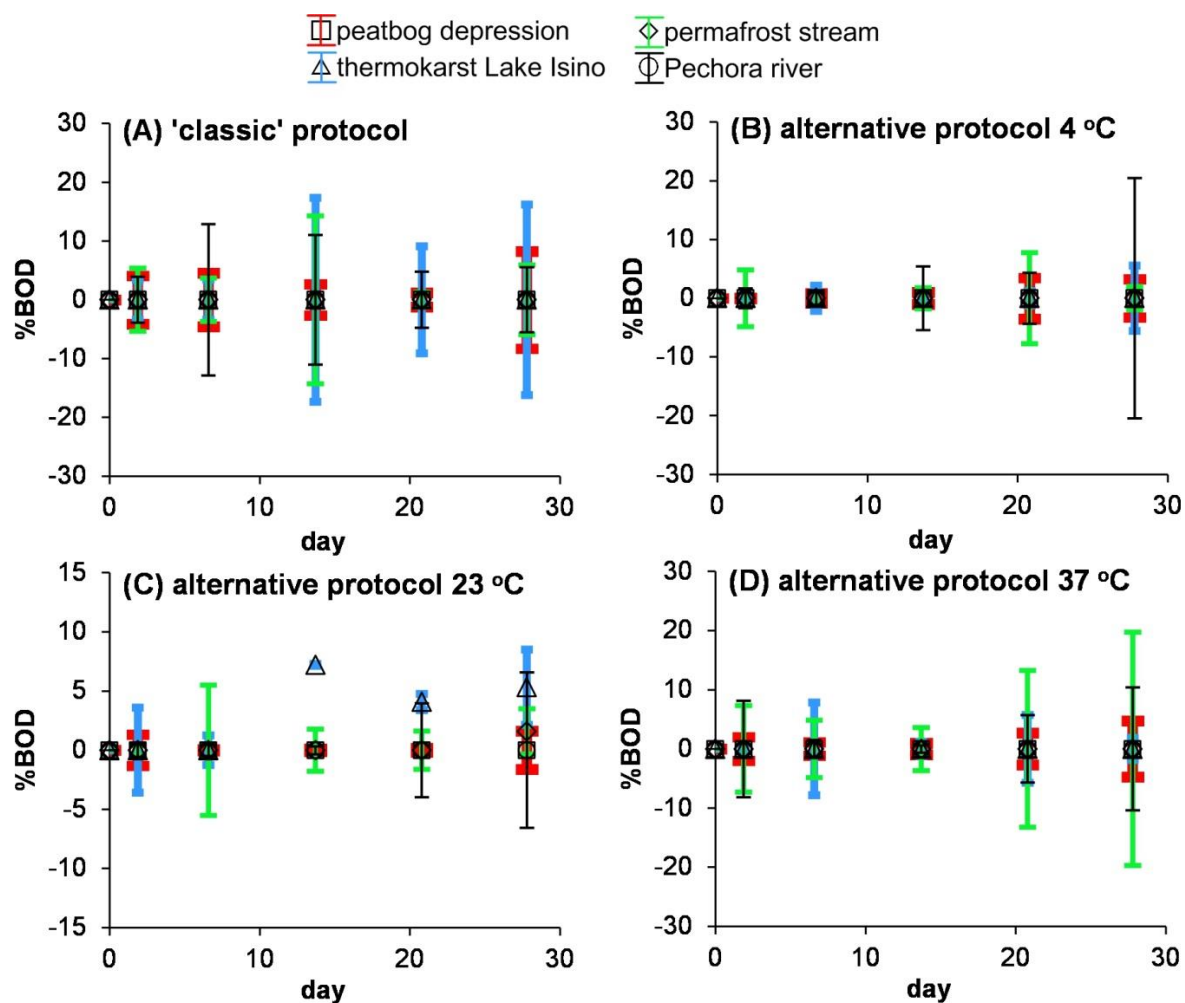
935 **Fig. 1.** The DOC concentration over time in biodegradation experiments at 23°C. The
 936 experiments are shown by solid symbols and the control runs are shown by open symbols: red
 937 squares, peatbog depression; green diamonds, permafrost stream; blue triangles, thermokarst
 938 Lake Isino, and black circles, the Pechora River. The error bars represent 1 s.d. of three replicates
 939 and often within the symbol size.

940

941

942

943



944

945

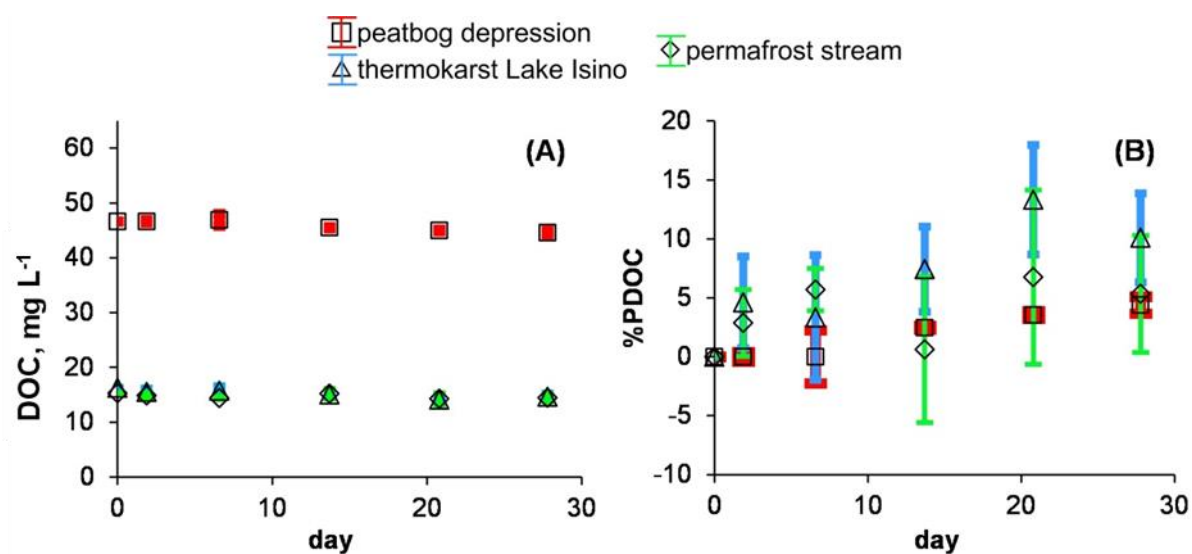
946

947 **Fig. 2.** Percentage of biodegradable DOC as a function of time. **A**, 'classic' protocol (0.7 μ m
948 GF/F filtration) at 23°C; **B-D**, alternative protocol of 3 μ m - filtered solution incubated at 4°C
949 (B), 23°C (C) and 37°C (D) and filtered through 0.22 μ m at each sampling. The error bars are 1
950 s.d. of triplicates or, in a few cases, duplicates.

951

952

953
954
955
956
957
958
959
960

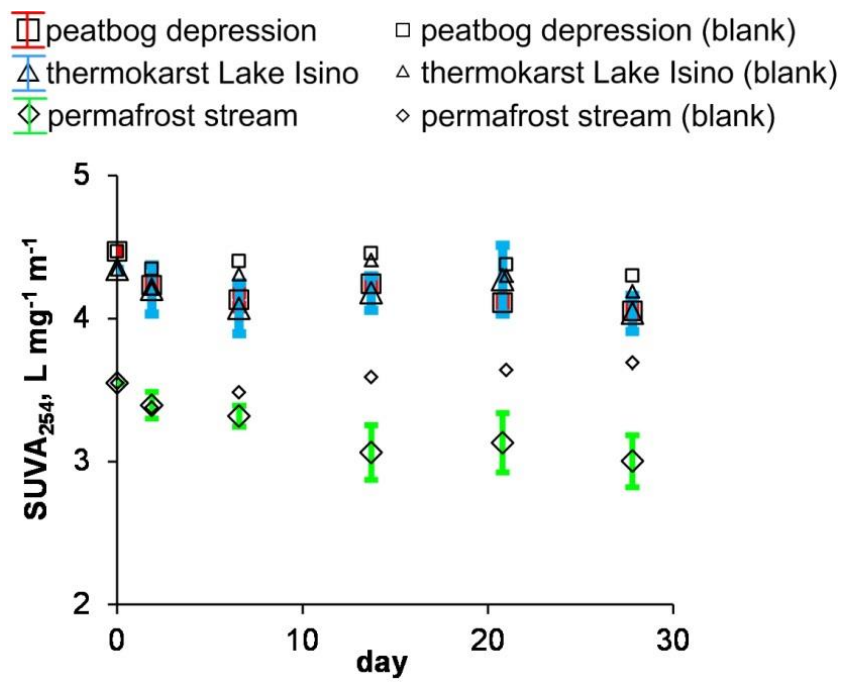


961
962
963

964 **Fig. 3.** Concentration (A) and percentage of degradable (B) DOC in photo-degradation
965 experiments. The experiments are shown by solid symbols and the control runs are shown by
966 open symbols: red squares, peatbog depression; green diamonds, permafrost stream; and
967 triangles, thermokarst Lake Isino. The error bars are 1 s.d. of triplicates.

968
969
970
971
972
973
974
975
976

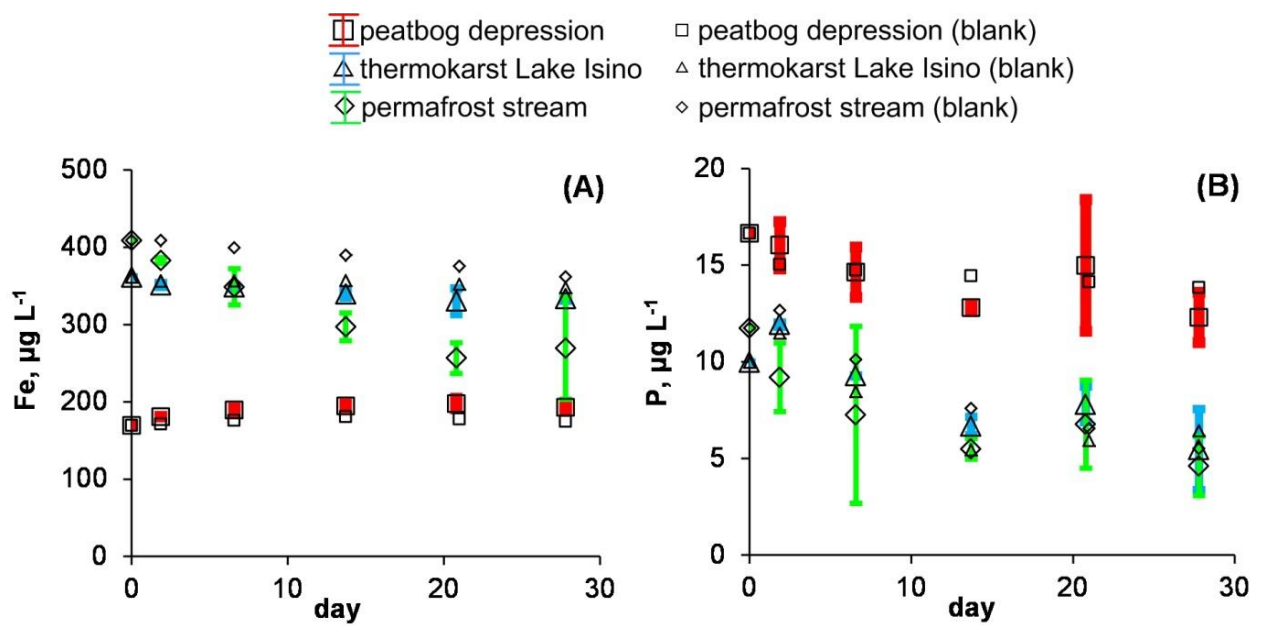
977
978
979
980
981
982
983
984
985
986
987
988
989
990



991
992
993
994
995
996
997
998
999
1000
1001
1002

Fig. 4. $SUVA_{254\text{ nm}}$ over time in photo-degradation experiments. The error bars are 1 s.d. of triplicates.

1003
1004
1005
1006
1007
1008
1009
1010
1011
1012
1013
1014
1015



1016
1017
1018
1019
1020
1021
1022
1023
1024
1025
1026

Fig. 5. Fe (A) and P (B) concentration over time in photo-degradation experiments. The error bars are 1 s.d. of triplicates.

1027 **Table 1.** Landscape setting, hydrochemical characteristics and CO₂ concentration and emission flux of studied waters. S.C. is specific
 1028 conductivity and TBC is total bacteria count (by DAPI).

Sample	BZ-2-17	BZ-24-17	BZ-12	P5
GPS coordinates	67°36'48,8"N, 53°54'29,8"E	67°36.53'N, 53°50.26'E	67°36'47,7"N, 53°54'38,5"E	67°40'09,4", 52°39'30,8"
Description	Depression in peatbog, S _{area} = 7.5 m ²	Stream in frozen peatland, S _{watershed} = 7.5 km ²	Thermokarst lake (Isino), S _{area} = 0.005 km ²	r. Pechora, S _{watershed} = 322,000 km ²
T, °C	24	25	24.1	20
pH	3.85	6.52	5.30	6.92
S.C., μS cm⁻¹	59.2	31.5	12.9	65.1
DOC, mg L⁻¹	43.9	16.6	15.6	8.20
DIC, mg L⁻¹	0.992	2.52	0.808	6.11
SUVA₂₅₄	4.08	3.32	4.10	3.82
P-PO₄, μg L⁻¹	2.3	9.8	4.4	26.7
P_{total}, μg L⁻¹	14.6	N.D.	7.3	37.5
N-NO₂, μg L⁻¹	14.6	5.0	3.6	1.67
N-NO₃, μg L⁻¹	14.6	N.D.	76.6	111
N-NH₄, μg L⁻¹	13	152	117	36.5
N_{total}, μg L⁻¹	228	N.D.	200	438
Si, μg L⁻¹	22	392	100	2690
TBC × 10⁶, cell mL⁻¹	0.81	5.72	5.36	3.51
pCO₂, ppm	440	2370	1200	1860 (night), 780 (day)
CO₂ flux, mmol m⁻² d⁻¹	34	30-300*	74	100-130*

1029
 1030 Footnote: *, by analogy with small streams of Western Siberian peatlands, of the discontinuous permafrost zone, located in similar
 1031 environmental context; ** By analogy with Taz and Pur Rivers of western Siberian peatlands (Serikova et al., 2018).

1032
 1033
 1034